# A feedback scheme for control of single electron transport

**Tobias Brandes**

TU Berlin, Institut für Theoretische Physik, Hardenbergstr. 36, D-10623 Berlin, Germany

Received XXXX, revised XXXX, accepted XXXX
Published online XXXX

**Key words:** Feedback control, single electron transport, quantum dots.

* Corresponding author: e-mail tobias.brandes@tu-berlin.de, Phone: +49-30-31423034

We revise a feedback control scheme for single electron transport. It is based on the idea of an adaptive modulation of the system parameters (such as tunnel rates) during the observation of the full counting statistics. This can be done via an iterative, step-wise modulation, or in a continuous manner. We compare these two procedures and discuss an extension of the previously used linear feedback protocol to the non-linear case. This involves an exponential dependence of tunnel rates on the differences $n - I_0 t$, where $n$ is the number of electrons transfered after time $t$ and $I_0$ the stationary target current. The feedback freezes the full counting statistics into a stationary distribution that we derive and analyse using a Fokker-Planck equation.



**1 Introduction** The feedback discussed here consists of an active scheme where measurement results are used to modulate system and/or bath parameters during the entire time evolution [1–5]. This clearly involves some intrinsically classical, stochastic signals even if the system to be controlled is fully quantum. In contrast, passive feedback [6] (not discussed here) is essentially the embedding of a (quantum) system into a larger (quantum) system such that effectively, some parts of the enlarged system control the original system, without the need of permanent, external observation [7–17] .

Recent experiments by the Hannover group [18] have successfully realized the first stable, fully controllable feedback loop based on the full counting statistics in a mesoscopic solid state systems, i.e., a quantum dot. The most exciting feature of their experiment was the freezing of the overall fluctuations of the electric current due to the feedback loop at large times. This effect had previously been predicted [19] in a simple feedback model of the full counting statistics $p(n,t)$, the probability of $n$ charges being transfered across the dot during a time interval $[0,t]$.

The experiment used an iterative, adaptive feedback scheme somewhat different from the original proposal but similar in spirit. Here, we re-analyse that scheme and it properties and compare with the original continuous (in time) control scheme.

The outline of this paper is as follows: after introducing the model in section 2, we derive cumulants and cumulant generating functions in section 3. A comparison with continuous feedback control is performed in section 4, including an analysis of strong feedback based on the Fokker-Planck equation. Section 5 gives a generalization to iteration schemes with more than one feedback parameter before we conclude in section 6.

**2 Model** We start with a stochastic model, where single particles move from a source into a drain reservoir at random times $t_i$. In the simplest case, this is defined as a Poissonian stochastic process starting at time $t = 0$ and described in terms of a probability

$$p_0(n,\gamma t) \equiv \frac{(\gamma t)^n}{n!} e^{-\gamma t}, \quad n = 0,1,2,\ldots \tag{1}$$

to find $n$ additional particles in the drain reservoir after time $t > 0$. Here, the only parameter is the rate $\gamma$ which usually has a fixed value. The probability $p_0(n,\gamma t)$ is the simplest example of what is called full counting statistics in the context of quantum transport: it describes, e.g., the statistics of unidirectional transport of quantized charges

(single electrons) through a single, strongly biased tunnel barrier.

Microscopically, the starting point is the system Hamiltonian $\mathcal{H}_{\rm S}$ of a few-state nanostructure weakly coupled to source (left L) and drain (right R) reservoirs (described by free fermion Hamiltonians $\mathcal{H}_\alpha = \sum_k \varepsilon_{k\alpha} c^\dagger_{k\alpha} c_{k\alpha}$, $\alpha$ =L/R) via the usual tunnel Hamiltonian $\mathcal{H}_T$. In second quantization,

$$\mathcal{H}_T = \sum_{k\alpha i} V_{k\alpha i} c_{k\alpha} d_i^\dagger + \text{H.c}, \tag{2}$$

with tunnel matrix elements $V_{k\alpha i}$ and the fermionic dot operators $d_i^\dagger$. The index $k$ can contain spin degrees of freedom. As $\mathcal{H}_{\rm S}$ typically contains interaction terms, the usual master equation approach starts from truncating the system Hilbert space to a few many-body states, based on which a master equation for the reduced dot density operator (valid for weak reservoir coupling at not too low temperatures $T$) is derived.

The simplest case is the non-interacting resonant level model (Fig. 1 with just one level only and assuming spin polarization), for which this approach yields a markovian rate equation defined by Golden Rule type rates $\Gamma_\alpha \equiv 2\pi \sum_k |V_{k\alpha}|^2 \delta(\varepsilon - \varepsilon_{k\alpha})$. These are assumed to be energy independent in the so-called flat-band limit, which together with the assumption of a large source-drain bias across the dot forms a simple but fairly good description of transport [18].

The single level model defined by the two rates $\Gamma_L$ and $\Gamma_R$ can be even further simplified in the limit of a strong asymmetry between the barriers, e.g. when $\Gamma_L \gg \Gamma_R$ allows for a time-scale separation of the two Poissonian processes. The transport properties are then effectively described by tracing out the dot degree of freedom, which leads to the single Poissonian process Eq. (1) with rate $\gamma \equiv \Gamma_R$ defining the full counting statistics of the system, cf. Fig. 1.

**2.1 Control options** Time-dependent control of transport in this simple model is now achieved by modifying the transition rate $\gamma$ (by gate voltages in the experiment [18]). This can be done in various ways. For example, instead of a fixed rate $\gamma$, one could have a time-dependent rate $\gamma = \gamma(t)$ ('open loop control'), or a rate $\gamma = \gamma(t_1, t_2, ..., t_n)$ that depends on an entire measurement record of all the times $t_i \leq t$. In the latter case, the future rates depend on the outcomes of previous measurement results, a situation which is called measurement-based feedback control.

Another feedback option is the form $\gamma = \gamma(n, t)$ where the rate is time-dependent as in open-loop control but depends on the previous stochastic events only via the cumulative variable $n$ [19]. In all these cases, the expressions for the probability distribution to find $n$ particles in the drain reservoir after time $t > 0$ will differ from the simple form Eq. (1). From the theoretical point of view, depending on the kind of 'control protocol' (i.e., the functional form of the rate $\gamma$), it can be very difficult to find closed expressions for this probability distribution [20].

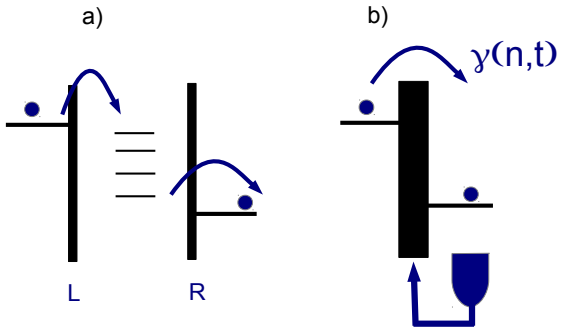


**Figure 1** a) Quantum dot coupled to reservoirs via left and right tunnel barriers. b) Simplified transport model after tracing out the dot, described by a single rate $\gamma(n, t)$ only. Feedback occurs by modulating the rate depending on the number of charges $n$ that have passed after a time $t$.

**2.2 Iterative feedback control** A powerful iterative feedback scheme has been experimentally tested recently [18]. The key idea there was to replace the time $t$ and the stochastic variable $n$ by an iteration index $i$ and the accumulated number of particles $N_i$, respectively. Here, $N_1, N_2, ...$ denote the number of electrons tunneled into the drain within the time intervals $[0, \Delta\tau], [\Delta\tau, 2\Delta\tau], ...$, where $\Delta\tau > 0$ is a fixed time interval window. The total number $n$ of electrons tunneled after, e.g., the time $t = k\Delta\tau$ has passed, is given by

$$n = N_1 + N_2 + ... + N_k. \tag{3}$$

Now, during the measurement, the rates are kept constant in each time interval and are only changed at times $t = i\Delta\tau$ according to the feedback protocol

$$\gamma_{i+1} = \gamma_i - \frac{\alpha}{\Delta\tau}(N_i - N_T). \tag{4}$$

This feedback protocol introduces two new control parameters; the dimensionless feedback strength $\alpha \geq 0$ and a target number $N_T$. Any deviation of the measured $N_i$ from the fixed target number $N_T$ thus leads to a correction of the old rate $\gamma_i$, with the correction being proportional to the deviation as govered by the feedback strength $\alpha$. For example, if there are too many electrons, $N_i - N_T > 0$, the new rate $\gamma_{i+1}$ is reduced. Note that $\alpha$ must not be too large here, as otherwise the rates would no longer be positive all the time. In the exponential feedback scheme discussed below, the restriction of small $\alpha$ will be removed.

After $k$ feedback iterations, we denote the probability at time $t = k\Delta\tau$ to have a measurement record of $N_1, ..., N_k$ particles tunneled in the respective time intervals by $p_k(N_1, ..., N_k)$. We start the counting at time $t = 0$

with a rate $\gamma_1$ and initially $n = N_0 = 0$ particles. The probability after the first ($k = 1$) time interval then is

$$p_1(N_1) = p_0(N_1, \gamma_1 \Delta\tau). \tag{5}$$

After the second interval, i.e. at time $t = 2\Delta\tau$, the new probability distribution is

$$p_2(N_1, N_2) = p_0(N_1, \gamma_1 \Delta\tau) p_0(N_2, \gamma_2 \Delta\tau). \tag{6}$$

Here, the factorization of $p_2$ into two distributions reflects the Markovian assumption that the counting within each time interval is governed by the same stochastic process, albeit with a renewed rate $\gamma_2$ for the second time window according to Eq. (4): $\gamma_2$ depends on $N_1$, which is why $N_2$ statistically depends on $N_1$.

Iteration of this procedure gives the simple product form

$$p_k(N_1, ..., N_k) = p_0(N_1, \gamma_1 \Delta\tau) ... p_0(N_k, \gamma_k \Delta\tau). \tag{7}$$

**2.3 Reduced probability** The probability distributions $p_k(N_1, ..., N_k)$ contain the full information concerning the measurement records in all the time windows. From a practical side, one might be more interested in the full counting statistics, i.e. the distribution $P(n, t)$ of the total particle number $n$ after time $t$, Eq. (3). At times $t = k\Delta\tau$, we obtain $P_k(n) \equiv P(n, k\Delta\tau)$ via the reduced probability

$$P_k(n) \equiv \sum_{N_1 ... N_k = 0}^{\infty} p_k(N_1, ..., N_k) \delta_{n, N_1 + ... + N_k}, \tag{8}$$

where $\delta_{n,n'}$ is the Kronecker symbol (unity if $n = n'$, zero else). Starting with $k = 1$ where

$$P_1(n) = p_1(N_1 = n) = p_0(n, \gamma_1 \Delta\tau), \tag{9}$$

we can iterate

$$\begin{aligned} P_{k+1}(n) &\equiv \sum_{N_1 ... N_{k+1}} p_k(N_1, ..., N_k) \delta_{n, N_1 + ... + N_{k+1}} \\ &\times p_0 \left( N_{k+1}, \left[ \gamma_1 - \frac{\alpha}{\Delta\tau} (N_1 + ... + N_k - k N_T) \right] \Delta\tau \right) \\ &= \sum_{N_{k+1}} P_k(n - N_{k+1}) \\ &\times p_0 \left( N_{k+1}, \left[ \gamma_1 - \frac{\alpha}{\Delta\tau} (n - N_{k+1} - k N_T) \right] \Delta\tau \right), \end{aligned} \tag{10}$$

where we could carry out all the $k$ sums over $N_1, ..., N_k$ since the arguments in $p_0$ depend on $N_{k+1}$ and $n - N_{k+1}$ only. Renaming the summation index $N_{k+1} \to n'$, this reads

$$\begin{aligned} P_{k+1}(n) = &\sum_{n'} P_k(n - n') \times \\ &\times p_0 \left( n', \gamma_1 \Delta\tau - \alpha \left( n - n' - k N_T \right) \right). \end{aligned} \tag{11}$$

This equation is our first key result. Note that in the derivation of Eq. (11), we do not require the specific Poissonian form Eq. (1) for the initial distribution $p_0$.

**3 Cumulants and feedback** In practice, it can be very difficult to obtain compact, analytical expressions for probability distributions that can be fitted to experimental data. Often it is easier to discuss moments or cumulants of a distribution rather than the distribution itself.

We now derive the first and second cumulants directly from Eq. (11) before turning to the more powerful cumulant generating function. In the following, we assume

$$\gamma_1 \Delta\tau = N_T \tag{12}$$

for simplicity. The initial rate $\gamma_1$ thus corresponds to a 'target current' of particles, which multiplied with the time window $\Delta\tau$ gives the desired target number $N_T$.

**3.1 First cumulant** The first cumulant of $P_k$ is just its first moment or the average number of transfered electrons after time $k\Delta\tau$,

$$\langle n \rangle_k \equiv \sum_{n=0}^{\infty} n P_k(n). \tag{13}$$

We multiply Eq. (11) with $n$ and carry out the sum to find

$$\langle n \rangle_{k+1} = \sum_m \sum_{n'} (m + n') P_k(m) \tag{14}$$

$$\times p_0 \left( n', N_T - \alpha(m - k N_T) \right), \tag{15}$$

where we used Eq. (12) and introduced the new variable $m \equiv n - n'$. Now, the first term in the sum $\propto m$ just gives $\langle n \rangle_k$ because the sum over $n'$ can be carried out and yields unity due to the normalisation of $p_0$. We thus can write

$$\begin{aligned} \langle n \rangle_{k+1} &= \langle n \rangle_k + \sum_m P_k(m) E_0 \left( N_T - \alpha(m - k N_T) \right) \\ E_0(\nu) &\equiv \sum_{n'} n' p_0(n', \nu), \end{aligned} \tag{16}$$

where we introduced the first cumulant $E_0(\nu)$ of the initial probability distribution that parametrically depends on $\nu$, the second argument in $p_0$. For a general distribution $p_0$, this dependence will be non-linear and as a consequence, Eq. (16) no longer leads to a closed equation for the first cumulants.

At this point, we return to our initial Poissonian model Eq. (1) which we use in the following. Its decisive advantage is the linearity of the expectation value $E_0(\nu)$, i.e.

$$E_0(\nu) = \nu, \quad \text{Poissonian.} \tag{17}$$

This immediately leads to an equation for the first moments only,

$$\langle n \rangle_{k+1} = N_T(1 + \alpha k) + (1 - \alpha) \langle n \rangle_k, \tag{18}$$

which is immediately solved by the strictly linear dependence in $k$,

$$\langle n \rangle_k = k N_T \tag{19}$$

under the initial condition $\langle n \rangle_0 = 0$. The average electron number is thus independent of the feedback strength $\alpha$ and is linearly increasing, as one expects by the defined target $N_T$.

**3.2 Second cumulant** The second cumulant is the variance of $P_k$ and uses the second moment $\langle n^2\rangle_k$,

$$C_2(k) \equiv \langle n^2\rangle_k - \langle n\rangle_k^2, \quad \langle n^2\rangle_k \equiv \sum_n n^2 P_k(n). \tag{20}$$

This quantity offers the best inside into the iterative feedback scheme and leads to most drastic deviations from the usual behaviour of the full counting statistics in absence of feedback.

We proceed as above but with $m+n'$ replaced by $(m+n')^2$. Again using the Poissonian model Eq. (1), we exploit the fact that all its cumulants are the same, and in particular

$$\sum_{n'} n'^2 p_0\,(n',\nu) = \nu + \nu^2, \quad \text{Poissonian.} \tag{21}$$

which we use for calculating the second moment $\langle n^2\rangle_{k+1}$ from Eq. (11). After some lengthy algebra, one finds

$$C_2(k+1) = C_2(k)(1-\alpha)^2 + N_T, \tag{22}$$

which has a solution given by the geometric series,

$$C_2(1) = N_T, \quad C_2(2) = N_T(1+(1-\alpha)^2)), ...$$
$$C_2(k) = N_T \sum_{n=0}^{k-1} (1-\alpha)^{2n}. \tag{23}$$

Without feedback, i.e. for $\alpha = 0$, this has the simple solution

$$C_2(k) = kN_T \quad \text{no feedback,} \tag{24}$$

which describes the usual spreading of the distribution function $P_k$ with a variance that increases linearly with time $t$ or iteration steps $k$ (with $C_2(k) = \langle n\rangle_k$ then for a Poissonian process).

This is drastically changed in presence of feedback $\alpha > 0$, as is most easily recognized in the long-time limit $k \to \infty$ of infinitely many iteration steps,

$$C_2(\infty) = \frac{N_T}{1-(1-\alpha)^2} = \frac{N_T}{\alpha(2-\alpha)}. \tag{25}$$

In presence of feedback, the variance thus no longer increases with $k$ but is *frozen in* at a constant value given by Eq. (25). This effect was first predicted in [19] and subsequently observed experimentally in [18].

The divergence of $C_2(\infty)$ at $\alpha = 2$ in Eq. (25) is related to a breakdown of the feedback model Eq. (4) with is linear in $\alpha$ and thus potentially can lead to negative, unphysical rates when $\alpha$ is too large. This can be avoided by using a properly defined dependence of the rates at stronger $\alpha$, for example an exponential dependence similar to that the continuous feedback model below, cf. Eq. (54). Mathematically, the particular value $\alpha = 2$ for the divergence in Eq. (25) is determined by the radius of convergence of the geometric series Eq. (23) for the iterated second cumulant $C_2(k)$, but we have so far not found a more intuitive or physical explanation for this particular value.

**3.3 Cumulant generating function** The cumulant generating function

$$\mathcal{F}_k(\chi) \equiv \log \sum_{n=0}^{\infty} P_k(n) e^{i\chi n} \tag{26}$$

contains properties of the full counting statistics in a form that is useful in many cases. The $n$th cumulants $C_n(k)$ (that generalize $C_2(k)$, Eq. (20), to higher $n$) are obtained from $\mathcal{F}_k(\chi)$ via differentiation with respect to the counting field $\chi$ as

$$C_n(k) \equiv (-i)^n \frac{\partial \mathcal{F}_k(\chi)}{\partial \chi^n}\bigg|_{\chi=0}. \tag{27}$$

As we will see in the following, similar to the second cumulant $C_2(k)$ all cumulants with $n \geq 2$ are frozen in at large $k$, i.e., they approach constant values instead of increasing linearly with time as without feedback. Only the first cumulant $\langle n\rangle_k = kN_T$, Eq. (19), increases linearly and remains unchanged. We first write

$$\mathcal{F}_{k+1}(\chi) = \log\Big[\sum_{mn'} e^{i\chi(m+n')} \times P_k(m) p_0\,(n', N_T(1+\alpha k) - \alpha m)\Big], \tag{28}$$

where we introduced the new variable $m = n - n'$. We can formally re-write this as

$$\mathcal{F}_{k+1}(\chi) = \log\Big[\sum_{m} e^{i\chi m} \times P_k(m) e^{f_0(\chi, N_T(1+\alpha k)-\alpha m)}\Big] \tag{29}$$

by defining the cumulant generating function $f_0$ of the initial distribution $p_0$,

$$f_0(\chi,\nu) \equiv \log \sum_n e^{i\chi n} p_0(n,\nu). \tag{30}$$

Now, as was already the case in the calculation of the second cumulant, little progress is made here unless one has an analytical expression for $f_0(\chi,\nu)$. Again, for the Poissonian case the situation is most simple as one has

$$f_0(\chi,\nu) = \nu\left(e^{i\chi}-1\right), \quad \text{Poissonian} \tag{31}$$

with a linear dependence on $\nu$. In Eq. (29), this leads to

$$\mathcal{F}_{k+1}(\chi) = N_T(1+\alpha k)\left(e^{i\chi}-1\right) + \mathcal{F}_k\left(\chi + i\alpha\left(e^{i\chi}-1\right)\right), \quad \text{Poissonian} \tag{32}$$

which is now a closed equation for the cumulant generating function.

Cumulants are now obtained by taking derivatives with respect to $\chi$ on both sides of Eq. (32) and using the definition Eq. (27). Specifically for the second and third cumulant, we obtain the closed equations

$$C_2(k+1) = N_T + [1-\alpha]^2 C_2(k) \tag{33}$$
$$C_3(k+1) = N_T - 3\alpha[1-\alpha] C_2(k) + [1-\alpha]^3 C_3(k),$$

with the first line reproducing Eq. (22).

**3.4 Co-moving frame** With only the first cumulant $\langle n\rangle_k = kN_T$, Eq. (19), increasing linearly, it is advantageous to transform into a frame moving together with $\langle n\rangle_k$. For the cumulant generating function, this is achieved by defining

$$F_k(\chi) \equiv \mathcal{F}_k(\chi) - i\chi\langle n\rangle_k, \tag{34}$$

where $F_k(\chi)$ is the cumulant generating function in the co-moving frame, where the corresponding first cumulant vanishes. The Taylor expansion of $F_k(\chi)$ in $\chi$ starts with quadratic terms. Upon inserting into Eq. (32) we obtain

$$F_{k+1}(\chi) = N_T\left(-i\chi + e^{i\chi} - 1\right) + F_k\left(\chi + i\alpha\left(e^{i\chi}-1\right)\right), \tag{35}$$

which is now a closed equation for the cumulant generating function in the co-moving frame. The nice feature of Eq. (35), as compared to Eq. (32), is the fact that we can immediately extract a stationary long time ($k\to\infty$) limit, since the coefficients in Eq. (35) no longer depend on $k$;

$$F_\infty(\chi) = N_T\left(-i\chi + e^{i\chi} - 1\right) + F_\infty\left(\chi + i\alpha\left(e^{i\chi}-1\right)\right), \tag{36}$$

First, this is a good starting point to reproduce previous results [19] for the stationary, feedback-frozen cumulants $C_n^\infty$ in the limit of small feedback strength $\alpha \ll 1$. We then can expand Eq. (36) to first order in $\alpha$ to obtain

$$C_n^\infty = -\frac{N_T}{\alpha}\frac{\partial^{n-1}}{\partial(i\chi)^{n-1}}\frac{i\chi}{e^{i\chi}-1}\bigg|_{\chi=0} = -\frac{N_T}{\alpha}B_{n-1}, \tag{37}$$

which holds for $n \geq 2$ and uses the definition of the Bernoulli numbers $B_n$. This co-incides with the results from our continuous feedback scheme that we discuss in the next section. We also recognize that for $n = 2$ with $B_1 = -\frac{1}{2}$ the second stationary cumulant Eq. (25) is reproduced in the limit $\alpha \ll 1$ that is assumed in Eq. (37).

**4 Continuous feedback control** We arrive at a continuous version of the iterative feedback scheme Eq. (4) by sending the time-window $\Delta\tau \to 0$. At the same time, from Eq. (4) we recognize that we simultaneously must have $\alpha \to 0$ in order to obtain a meaningful finite feedback parameter in that limit, which we define as

$$g \equiv \lim_{\Delta\tau,\alpha\to 0}\frac{\alpha}{\gamma_1\Delta\tau}, \tag{38}$$

where $\gamma_1$ is the initial rate without feedback control. Using the iterated result

$$\gamma_{k+1} = \gamma_1 - \frac{\alpha}{\Delta\tau}\left(n - kN_T\right) \tag{39}$$

that follows from Eq. (4) and Eq. (3), we now replace the iteration index $k$ by time via $t = k\Delta\tau$. Defining the time (and $n$) dependent rate $\gamma(n,t) \equiv \gamma_k$ then, in the limit $\Delta\tau \to 0$, $\alpha \to 0$ we obtain

$$\gamma(n,t) = \gamma_1\left(1 - g(n - \gamma_1 t)\right), \tag{40}$$

where we used $N_T = \gamma_1\Delta\tau$.

**4.1 Feedback rate equation** The explicit form Eq. (40) was the starting point for the continuous feedback scheme based on the feedback rate equation

$$\dot p(n,t) = -\gamma(n,t)p(n,t) + \gamma(n-1,t)p(n-1,t) \tag{41}$$

used in [19] for unidirectional transport through a single tunnel barrier. We now recover the cumulant generating function belonging to Eq. (41) from the discrete version by taking the limit of Eq. (32) in analogy to Eq. (38). Defining $\mathcal{F}(\chi,t) \equiv \mathcal{F}_k$ and using $\mathcal{F}_{k+1} = \mathcal{F}(\chi,t) + \Delta\tau\partial_t\mathcal{F}(\chi,t) + O(\Delta\tau)^2$, from Eq. (32) in the limit $\Delta\tau\to 0$, $\alpha\to 0$ we get

$$\frac{\partial}{\partial t}\mathcal{F}(\chi,t) = \gamma_1(1+g\gamma_1 t)\left(e^{i\chi}-1\right) + i\gamma_1 g\left(e^{i\chi}-1\right)\frac{\partial}{\partial\chi}\mathcal{F}(\chi,t). \tag{42}$$

As can be verified by differentiation with respect to time $t$, this is equivalent to the equation for the *moment* generating function $\rho(\chi,t) \equiv \sum_n p(n,t)e^{i\chi n} \equiv e^{\mathcal{F}(\chi,t)}$,

$$\dot\rho(\chi,t) = \gamma_1\left(e^{i\chi}-1\right)\left(1 + g\left(t\gamma_1 - \frac{\partial}{\partial i\chi}\right)\right)\rho(\chi,t) \tag{43}$$

which was first derived in [19] for the continuous feedback scheme, together with the limiting values at $t\to\infty$ for the cumulants, Eq. (37) with $\frac{N_T}{\alpha}\to\frac{1}{g}$ and Eq. (38), thus

$$C_n^\infty = -\frac{1}{g}B_{n-1}. \tag{44}$$

This proves that indeed the continuous feedback scheme is naturally contained in the iterative version without any approximation other than the joint limits $\Delta\tau\to 0$, $\alpha\to 0$, Eq. (38).

The stationary cumulant generating function in the co-moving frame for the continuous scheme is defined as

$$F_\infty^{\rm c}(\chi) \equiv \lim_{t\to\infty}\left(\mathcal{F}(\chi,t) - i\chi\gamma_1 t\right). \tag{45}$$

Note that due to the term $-i\chi\gamma_1 t$ this function is no longer $2\pi$–periodic. Its explicit form is obtained via Eq. (42), which leads to a differential equation for $F_\infty^{\rm c}(\chi)$,

$$\frac{\partial}{\partial\chi}F_\infty^{\rm c}(\chi) = \frac{1}{ig}\left[-1 + \frac{i\chi}{e^{i\chi}-1}\right]. \tag{46}$$

Note that this no longer depends on the initial rate $\gamma_1$. Eq.(46) has the solution

$$F_\infty^{\rm c}(\chi) = \frac{1}{g}\left(i\chi - {\rm Li}_2\left(1-e^{-i\chi}\right)\right) \tag{47}$$

with the Dilogarithm function ${\rm Li}_2(z) \equiv \int_z^0 \frac{dt}{t}\ln(1-t)$, which is easily verified by differentiation with respect to $\chi$ and using $\frac{\partial}{\partial\chi}F_\infty^{\rm c}(0) = 0$ since we are in the co-moving frame.

**4.2 Fokker-Planck equation and nonlinear feedback** Further progress with the analysis of the feedback rate equation Eq. (41) is made by mapping it onto the corresponding Fokker-Planck equation. This can be done under the simplifying assumption that the number $n$ be made a continuous variable, which allows a Taylor expansion in $n$ of the terms $\gamma(n-1,t)p(n-1,t)$ in Eq. (41) leading to derivatives of these functions with respect to $n$.

We now also allow for bidirectional transport at finite bias by including the backward processes that are described by backwards rates $\bar{\gamma}(n,t)$. Truncation at the second order of the Taylor expansion, we arrive at the usual Fokker-Planck equation,

$$\dot{p}(n,t) = -\frac{\partial}{\partial n} j(n,t) \tag{48}$$

$$j(n,t) \equiv f(n-I_0 t)p(n,t) - \frac{\partial}{\partial n}\left[D(n-I_0 t)p(n,t)\right]$$

with the force and diffusion functions;

$$f(n) \equiv \gamma(n) - \bar{\gamma}(n), \quad D(n) \equiv \frac{1}{2}\left[\gamma(n) + \bar{\gamma}(n)\right]. \tag{49}$$

Here, $I_0$ denotes the target current such that the arguments of $f$ and $D$ vanish in Eq. (48) whenever $n = I_0 t$. In the following, we also generalize the linear feedback form Eq. (40) to an arbitrary functional dependence ('feedback protocol') of the rates on the difference $n - I_0 t$. The dependence on the single argument $n - I_0 t$ in the force and diffusion functions in Eq. (48) then allows for a great simplification: this is achieved by Galilei transforming into the co-moving frame, regarding $n$ as a position variable and by defining

$$\tilde{p}(n,t) \equiv p(n + I_0 t, t). \tag{50}$$

Inserting this into Eq. (48) yields a Fokker-Planck equation $\dot{\tilde{p}}(n,t) = -\frac{\partial}{\partial n}\tilde{j}(n,t)$ with time-*independent* drift and diffusion terms in the probability current $\tilde{j}(n,t)$,

$$\tilde{j}(n,t) = \left(f(n) - I_0\right)\tilde{p}(n,t) - \frac{\partial}{\partial n}\left[D(n)\tilde{p}(n,t)\right]. \tag{51}$$

The stationary, feedback frozen distribution

$$p_{\rm st}(n) \equiv \lim_{t\to\infty} \tilde{p}(n,t) \tag{52}$$

is then obtained by setting $\tilde{j}(n,t)$ in Eq. (51) zero, and by simple integration we find the stationary distribution

$$p_{\rm st}(n) \propto \frac{1}{D(n)} \exp\left[\int^n dn' \frac{f(n') - I_0}{D(n')}\right]. \tag{53}$$

This distribution still has to be normalized which is why the lower limit of the integral in the exponent is not specified in Eq. (53).

**4.3 Bidirectional feedback with exponential rates** It turns our that the Fokker-Planck equation is quite versatile as a tool to analyse various properties of the feedback process. In particular, with Eq. (53) we are now in a position to make predictions for stationary distributions $p_{\rm st}(n)$ as a result of a large class of feedback protocols. Among those, the exponential form

$$\gamma(n) = \gamma_+ e^{-gn}, \quad \bar{\gamma}(n) = \gamma_- e^{gn}, \quad g \geq 0 \tag{54}$$

is a convenient choice to make analytical progress, and it guarantees positivity of the rates at all feedback strengths $g$ (which are chosen symmetrically for forward and backward processes, i.e. $-g$ and $+g$ in the exponents in Eq. (54)). Here, $\gamma_\pm$ are the bare forward and backward rates without feedback which are related to each other via detailed balance,

$$\frac{\gamma_-}{\gamma_+} = e^{-\mathcal{A}}. \tag{55}$$

If the source and drain reservoir have identical temperature $T$ and are biased by the voltage drop $V$, the affinity $\mathcal{A}$ in Eq. (54) is given by

$$\mathcal{A} \equiv \frac{V}{k_B T}, \tag{56}$$

but we can also use $\mathcal{A}$ to describe, e.g., a thermal bias.

In the following, we set the target current $I_0$ to the current at no feedback $g = 0$,

$$I_0 = \gamma_+ - \gamma_-. \tag{57}$$

This has the advantage to eliminate one free parameter, and is also useful in the linear response discussion below, $I_0 = 0$ at $\mathcal{A} = 0$.

In fact, at $\mathcal{A} = 0$ the feedback then operates with time-independent rates in Eq. (48), i.e., lab-frame and co-moving frame coincide. No current is flowing then, but the feedback works in a constructive way in that it stabilizes the distribution $p(n,t)$. At large times, the stationary distribution is found from Eq. (53) as

$$p_{\rm st}(n) = \frac{g\Gamma\left(1+\frac{1}{g}\right)}{\sqrt{\pi}\Gamma\left(\frac{1}{2}+\frac{1}{g}\right)} \left(\cosh(gn)\right)^{-\frac{2}{g}-1}, \quad \mathcal{A} = 0, \tag{58}$$

where $\Gamma(.)$ denotes the Gamma function.

In the opposite case of infinite bias (infinite affinity), we find

$$p_{\rm st}(n) = \frac{4^{1/g} g^{1-\frac{2}{g}}}{\Gamma\left(\frac{2}{g}\right)} e^{(2+g)n - \frac{2}{g}e^{gn}}, \quad \mathcal{A} = \infty. \tag{59}$$

The corresponding stationary cumulant generating function is found by Fourier transformation as

$$F_\infty(\chi) = i\chi\frac{\log\frac{g}{2}}{g} + \ln\frac{\Gamma\left(1+\frac{2+i\chi}{g}\right)}{\Gamma\left(1+\frac{2}{g}\right)}, \quad \mathcal{A} = \infty, \tag{60}$$

and the cumulants are given in terms of derivatives of the Digamma function $\Psi(.)$,

$$C_n^\infty = \frac{1}{g^n}\Psi^{(n-1)}\left(1+\frac{2}{g}\right), \quad \mathcal{A} = \infty, \quad n \geq 2. \tag{61}$$

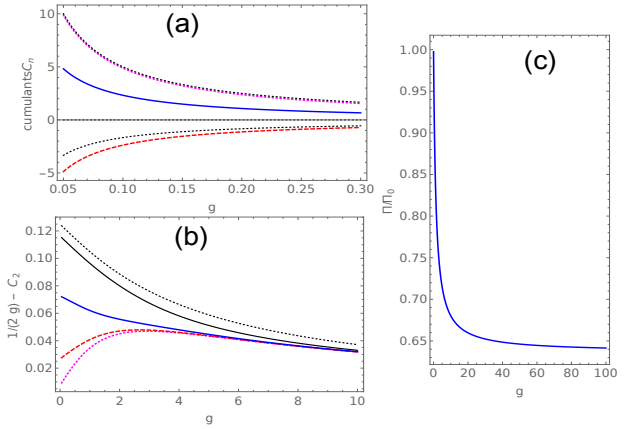


**Figure 2** Exponential feedback with rates Eq. (54) for single barrier (Poisson process). (a) Stationary frozen cumulants $C_2^\infty$ (magenta dotted), $C_3^\infty$ (red dashed) and $C_4^\infty$ (blue), Eq. (61), and their linear feedback counterparts, Eq. (44) (black dots) at infinite bias (affinity $\mathcal{A} \to \infty$). (b) Difference between $1/(2g)$ (linear feedback value at $\mathcal{A} = \infty$) and stationary second cumulants $C_2$ at affinity $\mathcal{A} = 0.5$ (magenta, dotted), 1 (red, dashed), 2 (blue), 4 (black), and 8 (black, dotted). (c) Feedback cooling effect: entropy production rate $\Pi$ divided by its zero feedback ($g = 0$, Joule heat) value $\Pi_0$ in the linear response regime $\mathcal{A} \to 0$, Eq. (67).

Numerically, the second cumulant $C_2^\infty$ of the exponential feedback model is very close to $1/(2g)$, the value from the rate equation based linear feedback model, Eq. (44), at basically the whole range of feedback strengths $g$, which is quite surprising. Deviations, however, become larger for higher cumulants as shown in Fig. 2a, for example for the fourth cumulant where the linear feedback model, Eq. (44), gives $C_4^\infty = 0$.

At finite affinities $\mathcal{A} > 0$, it is still possible to obtain an analytical expression in Eq. (53) which can then be used to calculate the normalization and the moments numerically. For the second cumulants, all the results are again close to the value $1/(2g)$. Fig. 2b therefore displays the differences to that value as a function of feedback strength $g$ for various affinities $\mathcal{A}$. Experimentally, it should be possible to test these deviations by tuning the bias voltage to smaller values.

**4.4 Entropy production rate** The perhaps most interesting application of the above Fokker-Planck equation is the analysis of entropy production and heat flow during the feedback process. The traditional discussion of these quantities in stochastic thermodynamics assumes a splitting into system and reservoir degrees of freedom [21]. In our case here, for the simple Poissonian case (single barrier between two reservoirs) there is no 'system' (like a quantum dot) in the usual sense. Instead, we are directly dealing with the numbers $n$ of transfered particles, which we can regard as the (system) degrees of freedom of a counting device.

We can then define the system Shannon $S(t)$ entropy as usual, i.e. as the Shannon entropy of the full counting statisics $p(n,t)$,

$$S(t) \equiv -\int dn p(n,t) \ln p(n,t), \tag{62}$$

where we already adopted the continuum description for $n$. Taking the temporal derivative, this leads to a continuity equation

$$\dot{S}(t) + \Phi(t) = \Pi(t), \tag{63}$$

where $\Phi(t)$ denotes the entropy flow and $\Pi(t)$ the rate of entropy production [22]. The physical picture here is very much like in other continuity equations, where the amount of some quantity $Q(= S)$ inside a region of space changes by the flow $\Phi$ of that quantity out of that region, and the production (or destruction) of $Q$ there. For a conserved quantity like charge, the right hand side in Eq. (63) is zero, but for the Shannon entropy a simple calculation based on the Fokker-Planck equation Eq. (48) proves the positivity of the entropy production rate,

$$\Pi(t) \equiv \int dn \frac{j(n,t)^2}{D(n - I_0 t)p(n,t)} \geq 0. \tag{64}$$

Now, in general $\Pi(t)$ may be hard to evaluate, as it requires the full time-dependent solution $p(n,t)$. However, things simplify again drastically in the long-time limit where we already anticipate the stationary, feedback frozen distribution $p_{\rm st}(n)$, Eq. (53). In fact, as we have $\tilde{j}(n, t \to \infty) = 0$ in the co-moving frame, in the lab frame this means $j(n,t) = \tilde{j}(n,t) - I_0 p(n,t)$ by virtue of Eq. (48), Eq. (51) and Eq. (50). At large times, therefore, we have $j(n, t \to \infty) = -I_0 p(n, t \to \infty)$ and thus

$$\Pi \equiv \lim_{t\to\infty} \Pi(t) = I_0^2 \int dn \frac{p_{\rm st}(n)}{D(n)}. \tag{65}$$

With $S(t \to \infty) = -\lim_{t\to\infty} \int dn p(n + I_0 t, t) \ln p(n + I_0 t, t) = -\int dn p_{\rm st}(n) \ln p_{\rm st}(n)$, the temporal change of the Shannon entropy vanishes and we have the stationary result $\Pi = \Phi \equiv \lim_{t\to\infty} \Phi(t)$. Then, there is an exact compensation: the generation of entropy per unit time $\Pi > 0$ in the detector is compensated by an equal amount of entropy flow $\Phi$ from the detector into the environment.

In an electronic transport situation, this flow is nothing but the Joule heat generated by a stationary current $I_0$ at a finite bias, albeit in presence of feedback. Without feedback, we thus expect Eq. (65) to reduce to the well-known expression $P = I_0 V$ for the dissipated power in a circuit. Using $I_0 = \gamma_+ - \gamma_-$ and detailed balance, Eq. (55), in that case $\Pi$ reduces to

$$\Pi_0 \equiv \frac{2I_0^2}{\gamma_+ + \gamma_-} = 2I_0 \tanh\left(\frac{1}{2}\mathcal{A}\right). \tag{66}$$

The maximum entropy production rate across the single barrier thus is $\Pi_0 = 2I_0$ at $\mathcal{A} = \infty$, but at small affinities $\mathcal{A} = V/(k_B T)$ the heat flow $P \equiv k_B T \Pi_0$ becomes indeed Joule's expression $P = I_0 V$.

Now, Eq. (65) also contains the corresponding expression at finite feedback. At small affinities, we obtain $\Pi$ by evaluating the expectation value $\langle \frac{1}{D(n)} \rangle$ in Eq. (65) with the stationary distribution $p_{\rm st}(n)$ evaluated for $\mathcal{A} = 0$, using the explicit expression Eq. (58). The result is a $g$-dependent reduction of the entropy production in this linear response regime, as expressed by

$$\frac{\Pi}{\Pi_0} = \frac{\left[\Gamma\left(1+\frac{1}{g}\right)\right]^2}{\Gamma\left(\frac{1}{2}+\frac{1}{g}\right)\Gamma\left(\frac{3}{2}+\frac{1}{g}\right)} \leq 1, \quad \mathcal{A} \to 0, \tag{67}$$

as shown in Fig. 2c. This can be interpreted as a feedback cooling effect. The limiting value of this cooling at very strong feedback $g \to \infty$ is a reduction by $\Pi/\Pi_0 = 2/\pi \approx 64\%$. As a remark here, we note that ultimately, the modification of the heat flow due to our active feedback scheme has to be understood to stem from the feedback loop. In our model, which uses time-dependent rates, this is not explicitely included. This is in contrast to passive feedback models, where (at least in principle) a more complete picture in terms of heat and information flowing in the entire system [21,23] can be given.

In the opposite limit of large affinity $\mathcal{A} \to \infty$, though, using Eq. (59) we find

$$\frac{\Pi}{\Pi_0} = 1 + \frac{g}{2}, \quad \mathcal{A} \to \infty. \tag{68}$$

We note that the values for $\Pi$ depend on our choice of $I_0$, Eq. (57), as our stationary target current. Using a different target current $I_0 \neq \gamma_+ - \gamma_-$ introduces a further, independent parameter into the analysis and the results for $\Pi$ are modified. For example, we could use the feedback to generate a finite target current $I_0$ at zero bias voltage $V = 0$ by employing our scheme with rates $\gamma_+ = \gamma_- \equiv \gamma_0$ in Eq. (54). This would amount to a pumping effect, with a finite dissipative entropy production at rate $\Pi = I_0^2/\gamma_0$ in lowest order of the feedback strength $g$.

**5 Beyond the Poissonian case** So far, all of our results have been based upon the simple Poissonian single barrier model. Clearly an extension to the more general case is desirable, for example by allowing to include internal degrees of freedom of a quantum dot through which the transport occurs.

**5.1 Multi-rate iteration scheme** We therefore generalize the iteration Eq. (4) by assuming a scheme

$$\boldsymbol{\gamma}_{i+1} = \boldsymbol{\gamma}_i - \frac{\boldsymbol{\alpha}}{\Delta\tau}(N_i - N_T) \tag{69}$$

that instead of depending on a single transfer rate depends on multiple rates, written as a vector $\boldsymbol{\gamma}_i$, in each iteration step $i$. Correspondingly, to each rate belongs one component of the feedback vector $\boldsymbol{\alpha}$. The initial probability density $p_0(n', \boldsymbol{\nu})$ in Eq. (11) then depends on vectors instead of scalars in its second argument, as is the case for its cumulant generating $f_0(\chi, \boldsymbol{\nu})$ in Eq. (30). The assumption for the following is that we can still assume the factorized form Eq. (7) for the probability of a measurement record of $N_1, ..., N_k$ particles,

$$p_k(N_1, ..., N_k) = p_0(N_1, \boldsymbol{\gamma_1}\Delta\tau)...p_0(N_k, \boldsymbol{\gamma}_k\Delta\tau). \tag{70}$$

We then have to replace Eq. (29) by

$$\mathcal{F}_{k+1}(\chi) = \log\Big[\sum_m e^{i\chi m} \times P_k(m) e^{f_0(\chi, \boldsymbol{\gamma}_1\Delta\tau + \boldsymbol{\alpha}(kN_T - m))}\Big]. \tag{71}$$

Progress can be made here for weak feedback, i.e. by expanding $f_0$ in $\boldsymbol{\alpha}$. We then obtain a closed expression for the cumulant generating function $\mathcal{F}$ in presence of feedback corresponding to Eq. (32),

$$\mathcal{F}_{k+1}(\chi) = f_0\left(\chi, \boldsymbol{\gamma}_1\Delta\tau\right) + kN_T\boldsymbol{\alpha}\nabla f_0(\chi, \boldsymbol{\gamma}_1\Delta\tau) + \mathcal{F}_k\left(\chi + i\boldsymbol{\alpha}\nabla f_0(\chi, \boldsymbol{\gamma}_1\Delta\tau)\right). \tag{72}$$

Here and in the following, the gradient $\nabla f_0$ refers to the second (vector) argument in $f_0$. Again assuming a first cumulant $\langle n \rangle = N_T k$ linearly increasing in $k$, we transform into the co-moving frame by defining $F_k(\chi)$ as in Eq. (34), where we obtain

$$F_{k+1}(\chi) = -i\chi N_T + f_0\left(\chi, \boldsymbol{\gamma}_1\Delta\tau\right) + F_k\left(\chi + i\boldsymbol{\alpha}\nabla f_0(\chi, \boldsymbol{\gamma}_1\Delta\tau)\right). \tag{73}$$

**5.2 Small feedback strength and second cumulant** Again expanding in $\boldsymbol{\alpha}$, we now find the equation for the stationary cumulant generating function in the co-moving frame as

$$\frac{\partial}{\partial\chi}F_\infty(\chi) = \frac{i\chi N_T - f_0\left(\chi, \boldsymbol{\gamma}_1\Delta\tau\right)}{i\boldsymbol{\alpha}\nabla f_0(\chi, \boldsymbol{\gamma}_1\Delta\tau)}. \tag{74}$$

Again, for simplicity we assume that the target number $N_T$ is initially fixed as the first cumulant without feedback, $N_T = -i\,\partial_\chi f_0\left(\chi, \boldsymbol{\gamma}_1\Delta\tau\right)|_{\chi=0}$. The numerator in Eq. (74) therefore is $O(\chi^2)$ whereas the denominator is $O(\chi)$, which means that $\partial_\chi F_\infty(\chi))|_{\chi=0} = 0$ as should be in the co-moving frame. Using $F_\infty(0) = 0$ we thus have the generalization of Eq. (47) in the formal result

$$F_\infty(\chi) = \int_0^\chi dx \frac{ixN_T - f_0\left(x, \boldsymbol{\gamma}_1\Delta\tau\right)}{i\boldsymbol{\alpha}\nabla f_0(x, \boldsymbol{\gamma}_1\Delta\tau)}. \tag{75}$$

As an application, we directly derive a formula for the second feedback stabilized cumulant $C_2^\infty$ from Eq. (74). It is useful to define the first cumulants $\kappa_n(\boldsymbol{\gamma}_1\Delta\tau) \equiv \partial_{i\chi}^n f_0(\chi, \boldsymbol{\gamma}_1\Delta\tau)\big|_{\chi=0}$ of the no-feedback system, by which the stationary $C_2^\infty$ follows as

$$C_2^\infty = \frac{\kappa_2(\boldsymbol{\gamma}_1\Delta\tau)}{2\boldsymbol{\alpha}\nabla\kappa_1(\boldsymbol{\gamma}_1\Delta\tau)}. \tag{76}$$

As an example, as in [19] we consider a single level quantum dot with left/right tunnel rates $\Gamma_{L/R}$ in $\boldsymbol{\gamma}_1 = (\Gamma_R, \Gamma_L)$, an asymmetry parameter $a$ defined via $\Gamma_R = \Gamma_L\frac{1-a}{1+a}$, and a corresponding feedback scheme with

strength $\boldsymbol{\alpha}/\Delta\tau = (\Gamma_R g_R, \Gamma_L g_L)$. Defining the asymmetry parameter $b$ for the feedback couplings correspondingly via $g_R = g_L \frac{1-b}{1+b}$, from Eq. (76) with $\kappa_1 = N_T = \Gamma_L \Delta\tau \frac{1-a}{2}$ and $\kappa_2 = \frac{1}{2}(1+a^2)N_T$, we find

$$C_2^\infty = \frac{1}{2g_L} \frac{(1+a^2)(1-a)}{\frac{1-b}{1+b}(1-a^2)+(1-a)^2}. \tag{77}$$

This fits the results obtained numerically in [19] and thus underlines the consistency of the iterative scheme with the continuous feedback scheme also for the multi-rate situation.

**6 Discussion** As it turns out, both the iterative and the continuous feedback schemes are mathematically very rich and leave many challenges and unanswered questions. First, it seems quite hard to go beyond linear feedback except in the continuous version. Even there, only the Fokker-Planck equation offers a fairly transparent analysis via the possibility to obtain stationary solutions. This can probably be generalized beyond the simple single Poissonian model, i.e. in situations with more internal system (dot) degrees of freedom.

Keeping the charge $n$ integer requires to use the full rate equation instead of the Fokker-Planck equation which describes $n$ as a continuous variable. For exponential rates, one can then derive the moment generating function in a moving frame and an infinite sequence of its values in the complex plane. Using this, one could then re-construct the full function and all the cumulants. This suggests that there are connections to problems in complex analysis, as is also indicated by the appearance of interesting functions such as the Dilogarithm function $\mathrm{Li}_2(z)$ [24], the Bernoulli numbers $B_n$ and the continuation from integers $n$ to numbers in the complex plane.

What is helpful in all the models discussed here is the dependence on $n - I_0 t$ of the control parameters (rates) which can always be removed by a Galilei transformation into a co-moving inertial system. It would be interesting to understand this feature from a more general point of view, perhaps with the perspective to introduce control into other equations (like wave equations), or even in a relativistic setting.

Physically, the freezing of the full counting statistics seems to be a robust feature independent of the particular implementation of a feedback protocol. An indication is the appearance of the $1/g$–dependence of the frozen second cumulant over and over again in the various analytical approaches, where $g$ is the feedback strength. But also the experiment itself leaves challenges for detailed theoretical analysis, e.g., the scaling form of the stationary, temporal fluctuations of the cumulants [18].

Also recently, we analysed a feedback control scheme for a correlation function in non-equilibrium, the waiting time distribution $w(\tau)$ [20]. It turns out that large feedback is required to achieve a noticeable control over the waiting times, in contrast to the long-time full-counting statitics discussed here where small values of $g$ are sufficient. It would be interesting to devise other and better control schemes that allow a simpler control of correlation functions.

Another bigger topic is the thermodynamic interpretation of feedback schemes [25–34, 21, 35–41]. We have recently suggested a Fokker-Planck based analysis of a corresponding passive feedback model consisting of many interacting channels [23], but the particular form of the interactions among the particles in the channels was rather artificial there. We therefore regard the derivation of the entropy production rate $\Pi$, Eq. (67), out of the original active feedback model as a step forward. Still, it would be desirable to better understand the relation between active and passive feedback models. One could also speculate that hybrids between active and passive feedback control should offer interesting new perspectives.

**Acknowledgements** I thank M. Esposito, C. Flindt, R. J. Haug, G. Kießlich, G. Schaller, P. Strasberg, and T. Wagner for valuable discussions, and acknowledge support by the DFG via projects BR 1528/7, 1528/8, 1528/9, SFB 910 and GRK 1558.

## References

[1] H. M. Wiseman and G. J. Milburn, *Quantum Measurement and Control* (Cambridge University Press, Cambridge, England, 2009).
[2] K. Jacobs, *Quantum Measurement Theory and Applications* (Cambridge University Press, Cambridge, 2014).
[3] J. Zhang, Y. Liu, R. Wu, K. Jacobs, F. Nori, arXiv:1407.8536 [quant-ph] (2014).
[4] C. Chen, L.-C. Wang, and Y. Wang, The Scientific World Journal **2013** 1 (2013).
[5] E. Schöll, S. H. L. Klapp, P. Hövel (Eds.), *Control of Self-Organizing Nonlinear Systems* (Springer International Publishing, 2016).
[6] C. Emary and J. Gough, Phys. Rev. B **90**, 205436 (2014).
[7] S. Lloyd, Phys. Rev. A **62**, 022108 (2000).
[8] J. Zhang, Y. Liu, R. Wu, C. Li, and T. Tarn, Phys. Rev. A **82**, 022101 (2010).
[9] Z. Liu, H. Wang, J. Zhang, Y. Liu, R. Wu, C. Li, and F. Nori, Phys. Rev. A **88** 063851 (2013).
[10] A. Carmele, J. Kabuss, F. Schulze, S. Reitzenstein, and A. Knorr, Phys. Rev. Lett. **110**, 013601 (2013).
[11] S. M. Hein, F. Schulze, A. Carmele, and A. Knorr, Phys. Rev. Lett. **113**, 027401 (2014).
[12] A. L. Grimsmo, A. S. Parkins, and B.-S. Skagerstam, New J. Phys. **16**, 065004 (2014).
[13] F. Schulze, B. Lingnau, S. M. Hein, A. Carmele, E. Schöll, K. Lüdge, and A. Knorr, Phys. Rev. A **89**, 041801(R) (2014).
[14] J. Kabuss, D.O. Krimer, S. Rotter, K. Stannigel, A. Knorr, and A. Carmele, Phys. Rev. A **92**, 053801 (2015).
[15] S.M. Hein, F. Schulze, A. Carmele, and A. Knorr, Phys. Rev. A **91**, 052321S (2015).
[16] A. L. Grimsmo, Phys. Rev. Lett. **115**, 060402 (2015).
[17] J. Kabuss, F. Katsch, A. Knorr, and A. Carmele, J. Opt. Soc. Am. B **33**, 7 FOP1 (2016).
[18] T. Wagner, J. C. Bayer, E. P. Rugeramigabo, P. Strasberg, T. Brandes, and R. J. Haug, Nature Nanotechnology (2016).

[19] T. Brandes, Phys. Rev. Lett. **105**, 060602 (2010).
[20] T. Brandes, C. Emary, Phys. Rev. E **93**, 042103 (2016).
[21] J. M. Horowitz, M. Esposito, Phys. Rev. X **4**, 031015 (2014)
[22] T. Tomé, Braz. J. Phys. **36**, 1285 (2006).
[23] T. Brandes, Phys. Rev. E **91**, 052149 (2015).
[24] D. Zagier, J. Math. Phys. Sci. **22**, 131(1988).
[25] T. Sagawa and M. Ueda, Phys. Rev. Lett. **100**, 080403 (2008).
[26] T. Sagawa and M. Ueda, Phys. Rev. Lett. **104**, 090602 (2010).
[27] J. Horowitz and J. M. P. Parrondo, Europhys. Lett. **95**, 10005 (2011).
[28] T. Sagawa and M. Ueda, Phys. Rev. E **85**, 021104 (2012).
[29] D. Abreu and U. Seifert, Phys. Rev. Lett. **108**, 030601 (2012).
[30] T. Munakata and M. L. Rosinberg, J. Stat.Mech. P05010 (2012).
[31] M. Esposito and G. Schaller, Europhys. Lett. **99**, 30003 (2012).
[32] J. M. Horowitz, T. Sagawa, and J. M. R. Parrondo, Phys. Rev. Lett. **111**, 010602 (2013).
[33] P. Strasberg, G. Schaller, T. Brandes, and M. Esposito, Phys. Rev. Lett. **110**, 040601 (2013).
[34] H. Tasaki, arXiv:1308.3776 (2013).
[35] D. Hartich, A. C. Barato, U. Seifert, J. Stat. Mech. P02016 (2014).
[36] A.C. Barato and U. Seifert, Phys. Rev. Lett. **112**, 090601 (2014).
[37] N. Shiraishi and T. Sagawa, Phys. Rev. E **91**, 012130 (2015).
[38] P. Strasberg, G. Schaller, T. Brandes, and C. Jarzynski, Phys. Rev. E **90**, 062107 (2014).
[39] J. M. Horowitz, J. Stat. Mech: Theor. Exp. P03006 (2015).
[40] J. M. Horowitz and K. Jacobs, Phys. Rev. Lett. **115**, 130501 (2015).
[41] J.V. Koski, A. Kutvonen, I.M. Khaymovich, T. Ala-Nissila, and J.P. Pekola, Phys. Rev. Lett. **115**, 260602 (2015).